# Synthesis, Structure, Absolute Configuration, and Conformational Analysis of ($S_{Co}$,($S$,$R$)$_P$,$S_C$)-($\eta^5$-Cp)Co(N–N*)(P(O)(Ph)(OMe)) and Their Precursor ($S_{Co}$,$S_C$)-[($\eta^5$-Cp)Co(N–N*)(PPh(OMe)$_2$)]$^+$I$^-$ (N–N* = Bidentate Schiff Base). Characterization of an Arbuzov Reaction Intermediate with a Strongly Nucleophilic Counterion

Zhongxin Zhou, Chet Jablonski,* and John Bridson[1]

*Department of Chemistry, Memorial University of Newfoundland, St. John's, Newfoundland, Canada A1B 3X7*

*Received February 2, 1993*®

Reaction of ((*S*,*R*)$_{Co}$,$S_C$)-($\eta^5$-Cp)Co(N–N*)(I) (N–N* = ($S_C$)-Ph(Me)C*H—N=CH—C$_4$H$_3$N$^-$, C$_4$H$_3$N$^-$ = pyrrolyl), **2a**/**2b** = 85/15, with PPh(OMe)$_2$ in benzene affords **3a**, ($S_{Co}$,$S_C$)-[($\eta^5$-Cp)Co(N–N*)(PPh(OMe)$_2$)]$^+$I$^-$, as a diastereomerically pure, air-stable, deep-red precipitate. The cationic phosphonite complex **3a** collapses with 100% retention at cobalt in a variety of aprotic solvents to give ($S_{Co}$,($S$,$R$)$_P$,$S_C$)-($\eta^5$-Cp)Co(N–N*)(P(O)(Ph)(OMe)), **4a**,**b**, with 30–36% de at phosphorus. The model complex, ($S_{Co}$,$S_C$)-[($\eta^5$-Cp)Co(N–N*)(PPhMe$_2$)]$^+$]$^-$, **5a**, was prepared in order to investigate the stereochemical stability of the Arbuzov reaction intermediate, **3a**. Absolute configurations of **3a**, **4a**·2H$_2$O, and **5a** were determined crystallographically, **3a** crystallizes in the orthorhombic system, space group $P2_12_12_1$ (No. 19) with $a$ = 13.77(2) Å, $b$ = 18.08(1) Å, $c$ = 10.862(6) Å, $V$ = 2705(4) Å$^3$, $Z$ = 4, and $R$ = 0.046 ($R_w$ = 0.041) for 962 reflections with $I > 3.00\sigma(I)$. **4a**·2H$_2$O crystallizes in the orthorhombic system, space group $P2_12_12_1$ (No. 19) with $a$ = 16.692(5) Å, $b$ = 32.33(2) Å, $c$ = 9.379(6) Å, $V$ = 5062(4) Å$^3$, $Z$ = 8, and $R$ = 0.065 ($R_w$ = 0.047) for 1112 reflections with $I > 3.00\sigma(I)$. **5a** crystallizes in the orthorhombic system, space group $P2_12_12_1$ (No. 19) with $a$ = 13.308(4) Å, $b$ = 17.977(4) Å, $c$ = 10.790(3) Å, $V$ = 2581(1) Å$^3$, $Z$ = 4, and $R$ = 0.065 ($R_w$ = 0.046) for 873 reflections with $I > 3.00\sigma(I)$. The absolute configuration of **4b** was assigned on the basis of circular dichroism spectra. $^1$H nuclear Overhauser effect difference (nOed) spectra show that the solid state conformations of **3a**, **4a**·2H$_2$O, and **5a** persist in solution. Kinetic studies of the Arbuzov dealkylation step, **3a** → **4a**,**b**, are consistent with an irreversible first order collapse of an ion pair in aprotic solvents. Dealkylation of **3a** does not proceed in methanol, which strongly solvates I$^-$.

## Introduction

Arbuzov-like reactions[2] of transition metal halides and phosphites have proven to be one of the most versatile pathways for the synthesis of metallophosphonates (L$_n$M–P(O)(OR)$_2$).[3–28] Although SET mechanisms have been claimed in the literature,[4] the majority of mechanistic studies show that transition metal Arbuzov-like dealkylation reactions proceed via an ionic mechanism,[4,5,9,13,15–21,23–26,29] cf. eq 1. Initial substitution of the L$_n$M–X halide by phosphite forms a cationic phosphite intermediate complex, [L$_n$M(P(OR)$_3$)]$^+$X$^-$. Subsequent

* Abstract published in *Advance ACS Abstracts*, August 15, 1993.

(1) Crystallography Unit, Department of Chemistry, Memorial University.

(2) Bhattacharya, A. K.; Thyagarajan, G. *Chem. Rev.* **1981**, *81*, 415–30.

(3) We have named the M–P(O)(OR)$_2$ (metallophosphonates) complexes as organometallic phosphonic acid esters (R'P(O)(OR)$_2$) and the M–P(O)R'(OR) (metallophosphinates) as organometallic secondary phosphinic acid esters (R'$_2$P(O)(OR)).

(4) Brill, T. B.; Landon, S. J. *Chem. Rev.* **1984**, *84*, 577–85.

(5) Haines, R. J.; DuPreez, A. L.; Marais, L. L. *J. Organomet. Chem.* **1971**, *28*, 405–13.

(6) Clemens, J.; Neukomm, H.; Werner, H. *Helv. Chim. Acta* **1974**, *57*, 2000–10.

(7) Harder, V.; Werner, H. *Helv. Chim. Acta* **1973**, *56*, 1620–8.

(8) Harder, V.; Dubler, E.; Werner, H. *J. Organomet. Chem.* **1974**, *71*, 427–33.

(9) King, R. B.; Diefenbach, S. P. *Inorg. Chem.* **1979**, *18*, 63–8.

(10) Newton, M. G.; Pantaleo, N. S.; King, R. B.; Diefenbach, S. P. *J. Chem. Soc., Chem. Commun.* **1979**, 55–6.

(11) Shakir, R.; Atwood, J. L.; Janik, T. S.; Atwood, J. D. *J. Organomet. Chem.* **1980**, *190*, C14–6.

(12) Bruce, M. I.; Shaw, G.; Stone, F. G. A. *J. Chem. Soc., Dalton Trans.* **1973**, 1667–72.

(13) Schubert, U.; Werner, R.; Zinner, L.; Werner, H. *J. Organomet. Chem.* **1983**, *253*, 363–74.

(14) Solar, J. M.; Rogers, R. D.; Mason, W. R. *Inorg. Chem.* **1984**, *23*, 373–7.

(15) King, C.; Roundhill, D. M. *Inorg. Chem.* **1986**, *25*, 2271–3.

(16) Kläui, W.; Buchholz, E. *Inorg. Chem.* **1988**, *27*, 3500–6.

(17) Nakazawa, H.; Kadoi, Y.; Mizuta, T.; Miyoshi, K.; Yoneda, H. *J. Organomet. Chem.* **1989**, *366*, 333–42.

(18) Nakazawa, H.; Kadoi, Y.; Miyoshi, K. *Organometallics* **1989**, *8*, 2851–6.

(19) Landon, S. J.; Brill, T. B. *J. Am. Chem. Soc.* **1982**, *104*, 6571–5.

(20) Towle, D. K.; Landon, S. J.; Brill, T. B.; Tulip, T. H. *Organometallics* **1982**, *1*, 295–301.

(21) Landon, S. J.; Brill, T. B. *Inorg. Chem.* **1984**, *23*, 4177–81.

(22) Landon, S. J.; Brill, T. B. *Inorg. Chem.* **1985**, *24*, 2863–4.

(23) Landon, S. J.; Brill, T. B. *Inorg. Chem.* **1984**, *23*, 1266–71.

(24) Sullivan, R. J.; Bao, Q. B.; Landon, S. J.; Rheingold, A. L.; Brill, T. B. *Inorg. Chim. Acta* **1986**, *111*, 19–24.

(25) Bao, Q. B.; Brill, T. B. *Inorg. Chem.* **1987**, *26*, 3447–52.

(26) Brunner, H.; Jablonski, C. R.; Jones, P. G. *Organometallics* **1988**, *7*, 1283–92.

(27) Jablonski, C. R.; Burrow, T.; Jones, P. J. *J. Organomet. Chem.* **1989**, *370*, 173–85.

(28) Jablonski, C. R.; Ma, H. Z.; Hynes, R. C. *Organometallics* **1992**, *11*, 2796–802.

(29) Neukomm, H.; Werner, H. *J. Organomet. Chem.* **1976**, *108*, C26–8.

0276-7333/93/2312-3677$04.00/0 

$$L_nM\text{—}X + P(OR)_3 \longrightarrow [L_nM\text{—}P(OR)_3]^+X^- \longrightarrow L_nM\text{—}\overset{O}{\overset{\|}{P}}(OR)_2 \quad (1)$$

collapse via halide attack at the $\alpha$-carbon of the coordinated phosphite releases alkyl halide and the metallophosphonate.

Cationic 18e ion-pair phosphite complexes of the form $[L_nM(P(OR)_3)]^+X^-$ (R = alkyl) are extremely labile with respect to Arbuzov-like dealkylation; hence relatively few examples have been isolated.[5,16-18,29,30] The first structurally characterized organometallic trimethyl phosphite Arbuzov intermediate was isolated by Brill[4,24] as a stable $PF_6^-$ salt.

Our studies[26-28,31] of chiral induction from the asymmetric metal center of pseudooctahedral cyclopentadienyl complexes in the Arbuzov-like dealkylation of Scheme I, concluded that reactivity and diastereoselectivity are subtly related to the stereoelectronic properties of the ligand sphere. Intramolecular hydrogen P=O···HNP bonding between the nascent phosphoryl oxygen and the aminophosphine was proposed to play a dominant role in controlling the observed chiral induction at prochiral coordinated phosphorus. We attempted to test this proposal by using blocked aminophosphine ligands PNR* (PNR* = (*S*)-$Ph_2PN(R)C^*H(Me)Ph$, R = $CF_3$, Me, $C_2H_5$, $CH_2Ph$) which could not hydrogen bond; however the Arbuzov sequence of Scheme I was unsuccessful.[28] In a search for alternative, non-hydrogen bonding supporting ligands we have now examined several chiral, bidentate, uninegative Schiff bases, N*–N⁻, first reported by Brunner.[32] Herein we report the resolution and X-ray crystallographic characterization of $(S_{Co},S_C)$-$[(\eta^5\text{-Cp})Co(N\text{–}N^*)(PPh(OMe)_2)]^+I^-$, **3a**, an example of an Arbuzov intermediate with a strongly nucleophilic counterion as well as its dealkylation which affords $(S_{Co},(S,R)_P,S_C)$-$(\eta^5\text{-Cp})Co(N\text{–}N^*)(P(O)(Ph)(OMe))$, **4a** and **4b**. The crystal structure of a model complex, $(S_{Co},S_C)$-$[(\eta^5\text{-Cp})Co(N\text{–}N^*)(PPhMe_2)]^+I^-$, **5a**, prepared in order to establish the stereochemical stability of Arbuzov intermediates, is also described. The structure, absolute configuration, and solution conformation of these complexes have been fully characterized using NMR, circular dichroism (CD), and crystallographic methods.

## Results and Discussion

**Synthesis and Characterization.** The synthesis of the complexes used in this study is summarized in Scheme II. Treatment of the diiodide **1** with N*–N (N*–N = (*S*)-$Ph(Me)C^*H\text{—}N{=}CH\text{—}C_4H_3N^-$, $C_4H_3N^-$ = pyrrolyl) in ether at room temperature[32] results in substitution of CO and $I^-$ to afford a black, crystalline solid, $((S,R)_{Co},S_C)$-$(\eta^5\text{-Cp})Co(N^*\text{–}N)(I)$, **2a,b**, with a **2a/2b** ratio of 85/15 (determined by integration of the $^1H$ NMR Me doublets at 1.80 and 2.19 ppm) in a chemical yield of 92%. Addition of a slight excess of $PPh(OMe)_2$ to a dark-blue, benzene solution of **2a,b** at room temperature resulted in the formation of an air-stable, deep-red precipitate. Simple filtration afforded a *single* diastereomer, **3a** (optical purity 98%), in 79% chemical yield. $^1H$ NMR analysis of the residue obtained by removing volatiles in vacuo from the filtrate showed six well-separated Cp singlets corresponding to both Co-epimeric phosphonite iodide salts, $((S,R)_{Co})$-$[(\eta^5\text{-Cp})Co(N\text{–}N^*)(PPh(OMe)_2)]^+I^-$, **3a** (5.40 ppm) and **3b** (5.67 ppm), and four diastereomeric phosphinate products $((S,R)_{Co},(S,R)_P)$-$(\eta^5\text{-Cp})Co(N\text{–}N^*)(P(O)(Ph)(OMe))$, **4a** (4.84 ppm), **4b** (4.71 ppm), **4c** (5.04 ppm), and **4d** (4.96 ppm).

The isolation of optically pure diastereomer **3a**, an intermediate with a strongly nucleophilic $I^-$ counterion, enabled us to unambiguously investigate Co* → P chiral induction in the ensuing Arbuzov dealkylation step (cf. discussion below). Complex **3a** is not air sensitive in the solid state or in solution; however facile nucleophilic attack of the $I^-$ counterion on the coordinated $PPh(OMe)_2$ occurs in a variety of aprotic solvents such as benzene, hexane, methylene chloride, chloroform, acetone, or acetonitrile at ambient temperature to give two of the four possible diastereomeric Arbuzov products, **4a** and **4b** (cf. discussion below). The ion-pair **3a** is surprisingly stable in methanol (<5% conversion after 24 h at 323 K), presumably reflecting the reduced nucleophilicity of strongly solvated $I^-$. This result shows clearly that free halide ion is required for the dealkylation.

Heating a suspension of **3a** in benzene at 60 °C resulted in loss of methyl iodide and quantitative formation of two P-epimeric phosphinate products, **4a** and **4b**, with 36% de at phosphorus and complete retention of stereochemistry at Co. Retention at the chiral metal shows (i) that substitution resistant **3a**[26,32-36] is configurationally stable at cobalt under Arbuzov reaction conditions and (ii) that, in contrast with other transition metal Arbuzov reactions,[4,19,21-23] substitution of $PPh(OMe)_2$ for $I^-$ is *not* reversible under the reaction conditions. The P-epimeric diastereomers **4a**·$2H_2O$ and **4b** are separated with difficulty as red, pastelike solids which are very stable both in the solid state and in solution, as observed in other metallophosphonate[18,19,28] and -phosphinate[37] complexes.

All complexes were characterized by $^1H$, $^{31}P\{^1H\}$, and $^{13}C\{^1H\}$ NMR. $^{31}P$ NMR spectra (Table I) showed characteristic singlets at 160.4 ppm (**3a**), 108.1 ppm (**4a**), and 101.6 ppm (**4b**) corresponding to coordinated phosphonite or phosphinate.[4] The $^1H$ NMR spectra of **3a**, **4a**, and **4b** (Table I) show distinct $\eta^5$-Cp, C*H, and C*–Me resonances typical for diastereomeric "piano-stool" complexes.[26-28,35] The diastereotopic dimethyl phenylphosphonite OMe groups in **3a** appear as two doublets at 4.05 and 3.82 ppm with $^3J_{PH}$ = 11.4 Hz. The phosphinate OMe group appears as a doublet at 3.55 ppm for **4a** and 3.45 ppm for **4b**.

The pyrrolyl ring protons, the ortho protons of C*–Ph in **3a** and the ortho, meta, and para protons of C*–Ph in **4a** are well resolved in all complexes and were assigned unambiguously on the basis of $^1H$ nuclear Overhauser effect difference (nOed) spectra (cf. Figures 1 and 2, and Scheme III). Spectra f, g, and h in Figure 1 allow assignment of the pyrrolyl protons in **3a**. Irradiation of the multiplet of H(4) (6.35 ppm, Figure 1g) shows strong enhancements to the resonances at 6.72 ppm (8.1%) and 7.30 ppm (8.8%), which are confidently assigned to H(3) and H(5). Spectrum f (Figure 1f) correlates the Cp signal at 5.35 ppm

(30) Sweigart, D. A. *J. Chem. Soc., Chem. Commun.* **1980**, 1159.
(31) Jablonski, C. R.; Ma, H. Z.; Chen, Z.; Hynes, R. C.; Bridson, J. N.; Bubenik, M. P. *Organometallics* **1993**, *12*, 917-26.
(32) Brunner, H.; Riepl, G.; Benn, R.; Rufinska, A. *J. Organomet. Chem.* **1983**, *253*, 93-115.
(33) Brunner, H.; Rambold, W. *J. Organomet. Chem.* **1974**, *64*, 373-83.
(34) Brunner, H. *Top. Curr. Chem.* **1975**, *56*, 67-90.
(35) Brunner, H. *Adv. Organomet. Chem.* **1980**, *18*, 151-206.
(36) Jablonski, C.; Zhou, Z.; Bridson, J. N. *J. Organomet. Chem.* **1992**, *429*, 379-89.
(37) Faure, B.; Archavlis, A.; Buono, G. *J. Chem. Soc., Chem. Commun.* **1989**, 805-7.

**Scheme I**

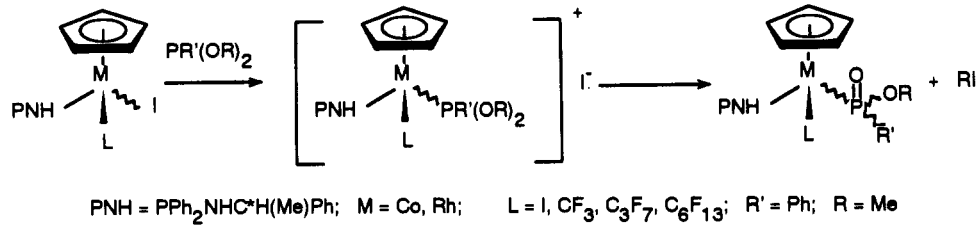


**Scheme II**

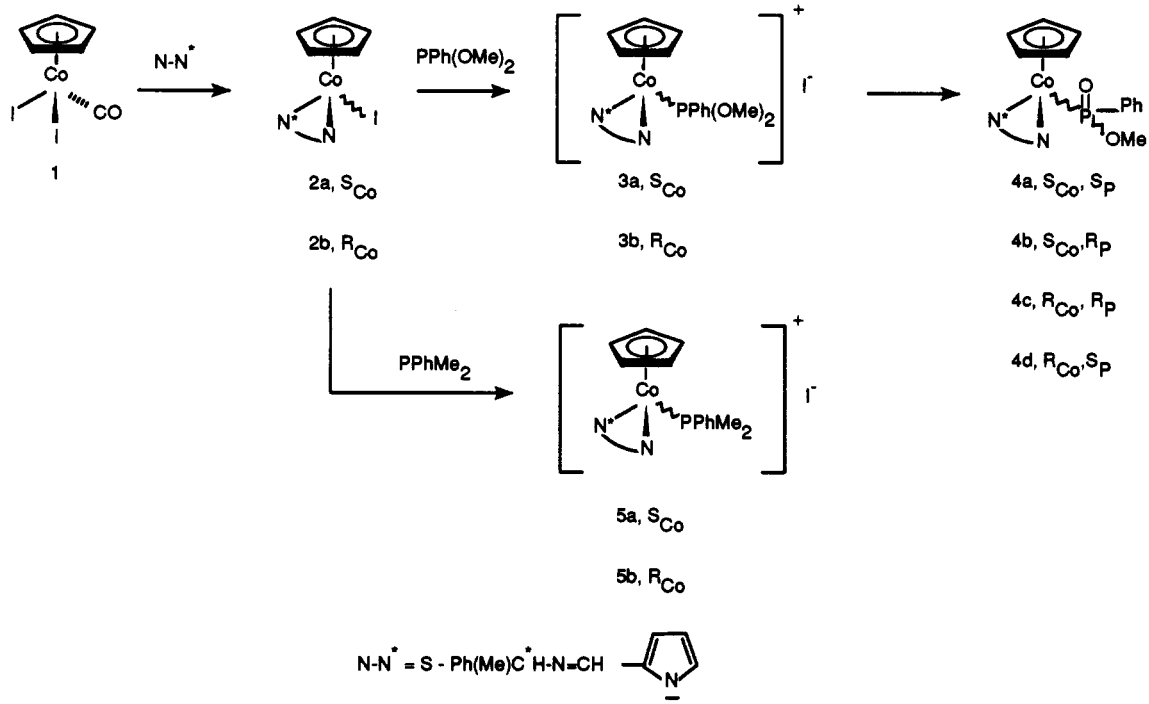


**Table I. $^1$H and $^{31}$P NMR for ($\eta^5$-Cp)Co(N–N*)(L) Complexes[a]**

| no. | Cp | H(3) | H(4) | H(5) | CH=N | C*H | POMe/PMe | C*Me | C*—Ph | P—Ph | $^{31}$P |
|---|---|---|---|---|---|---|---|---|---|---|---|
| **3a** | 5.40 (s) | 6.69 (m) | 6.37 (dd, 4.0, 1.9)[d] | *b* | *c* | 4.83 (q, 6.9)[e] | 4.17 (d, 11.4)[f]<br>3.90 (d, 11.4)[f] | 1.49 (d, 6.9)[e] | 7.05 (m)[g]<br>7.29–7.49 (m) | 7.29–7.49 (m) | 160.4 (s) |
| **3a**[h] | 5.35 (s) | 6.72 (dt, 4.0, 1.2)[i] | 6.35 (dd, 4.0, 1.9)[d] | 7.30[j] | 7.52[j] | 4.76 (q, 6.9)[e] | 4.05 (d, 11.3)[f]<br>3.82 (d, 11.4)[f] | 1.52 (d, 6.9)[e] | 7.06 (m)[g]<br>7.29–7.55 (m) | 7.29–7.55 (m) | |
| **4a** | 4.84 (s) | 6.51 (dt, 3.8, 0.6)[i] | 6.27 (dd, 3.9, 1.8)[d] | 7.15[k] | 7.06(d, 4.0) | 5.20 (q, 6.9)[e] | 3.55 (d, 11.0)[f] | 1.45 (d, 6.9)[e] | 7.15 (m)[l]<br>6.98 (t)[m]<br>6.97 (t)[m]<br>6.79 (dd)[n]<br>6.76 (dd)[n] | 7.30–7.37 (m) | 108.1 (s) |
| **4b** | 4.70 (s) | 6.72 (d, 3.8)[i] | 6.29 (m) | 7.02 | 7.47 (d, 3.6) | 5.22 (m) | 3.45 (d, 10.7)[f] | 1.68 (d, 6.9)[e] | 7.20–7.44 (m) | 7.20–7.44 (m) | 101.6 (s) |
| **5a** | 5.29 (s) | 6.88 (dt, 3.9, 1.0)[i] | 6.47 (dd, 4.0, 1.9)[d] | 7.20 | 7.56[j] | 5.23 (q, 6.9)[e] | 2.10 (d, 11.6)[o]<br>1.89 (d, 11.6)[o] | 1.52 (d, 6.9)[e] | 7.35–7.54 (m) | 7.35–7.54 (m) | 25.8 (s) |

[a] $^1$H (300, 1-MHz) NMR chemical shifts in ppm relative to internal TMS; $^{31}$P (121.5-MHz) NMR chemical shifts in ppm relative to external 85% $H_3PO_4$; solvent = $CDCl_3$; m = multiplet; s = singlet; d = doublet; t = triplet; q = quartet; $J$ values in Hz given in parentheses. [b,c] Overlapped with phenyl resonances. [d] ($^3J_{H(3)H(4)}$, $^3J_{H(5)H(4)}$). [e] $^3J_{HH}$. [f] $^3J_{PH}$. [g] $H_{ortho}$ (2H). [h] Solvent = $CD_3OD$. [i] ($^3J_{H(4)H(3)}$, $^4J_{HH}$). [j] Obtained from nOed spectra, overlapped with phenyl resonances. [k] Overlapped with $H_{para}$ on C*—Ph. [l] $H_{para}$. [m] $H_{meta}$ ($^3J_{HH}$ = 7.6). [n] $H_{ortho}$ ($^3J_{HH}$ = 8.4, $^4J_{HH}$ = 1.4). [o] $^2J_{PH}$.

with H(5) (8.4%), the proximal pyrrolyl proton, as shown in Scheme III, while spectrum h (Figure 1h) confirms the assignments of H(3) and H(4). The multiplet centered at 7.06 ppm is assigned to $H_{ortho}$ of C*–Ph on the basis of spectra b and e (Figure 1b,e), which show strong correlations between the $H_{ortho}$ and C*–Me as well as the $H_{ortho}$ and C*H.

The well-separated H(5) phenyl resonances (spectra e, f, and j in Figure 2) allow unambiguous assignment of the pyrrolyl protons in **4a**. Irradiation of H(4) at 6.27 ppm (Figure 2e) results in a strong enhancement of H(3) (6.51 ppm, 4.2%) and H(5) (7.15 ppm, 3.2%). Irradiation of H(3) (Figure 2f) shows a 5.2% enhancement of H(4) but no enhancement of H(5), while irradiation of H(5) (Figure 2j) shows 8.5% enhancement of H(4) but no enhancement of H(3).

$^1$H NMR assignments for **4b** were obtained by comparison with the spectra of **3a** and **4a**. In all complexes, as discussed above, the chemical shift of the pyrrolyl protons decreases in the order H(5) > H(3) > H(4), as found for other bidentate Schiff base complexes.[32] The chemical shift assignments of the C*–Ph $H_{ortho}$, $H_{meta}$, and $H_{para}$ in **4a** were based on spectra g′, h′, and j′ in Figure 2. Irradiation of $H_{meta}$ at 6.98 ppm (Figure 2h′) shows a

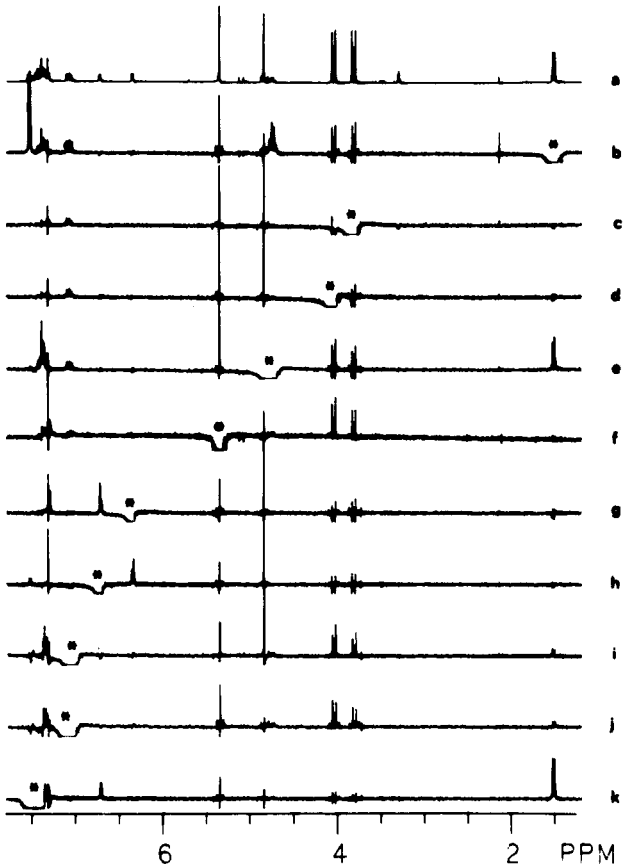


**Figure 1.** $^1$H nOed spectra of **3a** in $CD_3OD$: (a) reference spectrum; (b–k) difference spectra (×64) for irradiation at the indicated (*) frequency; (b) C*—Me; (c) & (d) P—OMe; (e) C*H; (f) Cp; (g) $H_4$; (h) $H_3$; (i) & (j) $H_{ortho}$ of C*—Ph; (k) Ph & CH=N.

large enhancement of the resonances at 7.15 ppm (4.2%) and 6.78 ppm (4.8%), which are then assigned to $H_{para}$ and $H_{ortho}$. The nOe correlation of the multiplet at 6.78 ppm with $H_{meta}$ (5.3%) and C*H (1.5%) but not with the multiplet at 7.15 ppm allows the assignment of the 6.78 ppm multiplet to $H_{ortho}$ on C*–Ph. Similarly, the multiplet at 7.15 ppm can be assigned to $H_{para}$ overlapped with H(5).

$^{13}$C NMR spectra (Table II) were analyzed using 2-D $^1$H/$^{13}$C $^1J$ heterocorrelation data which further confirm the $^1$H NMR assignments. All carbon signals were resolved and showed characteristic spectroscopic patterns for chiral phosphonite or phosphinate cyclopentadienyl complexes.[26] The two diastereotopic dimethyl phenylphosphonite OMe groups of **3a** are easily assigned as a pair of doublets at 57.30 and 57.12 ppm, respectively, with $^2J_{PC}$ = 13.2 Hz. The phosphinate OMe in **4a** and **4b** appears as a doublet at 51.67 ppm ($^2J_{PC}$ = 10.9 Hz) and 50.99 ppm ($^2J_{PC}$ = 11.9 Hz), respectively. All phenyl and pyrrolyl carbons were resolved and assigned unambiguously, as shown in Table II.

The model cationic phosphine complex, ($S_{Co}$,$S_C$)-[($\eta^5$-Cp)Co(N–N*)(PPhMe$_2$)]$^+$I$^-$, **5a**, originally isolated[32] as a Co-epimeric 88/12 **5a**/**5b** $PF_6^-$ salt mixture, was prepared in order to demonstrate the configurational stability at the Co center of the isostructural phosphonite complex **3a**. Treatment of a dark-blue solution of **2a**,**b** (**2a**/**2b** = 85/15) with excess PPhMe$_2$ following the procedure described for **3a** (Scheme II) gave a deep-red precipitate of optically pure diastereomer **5a** with the same configuration at Co as **3a** (cf. the discussion below) in 75% chemical yield. Heating solutions of **5a** in $CDCl_3$ at 60 °C

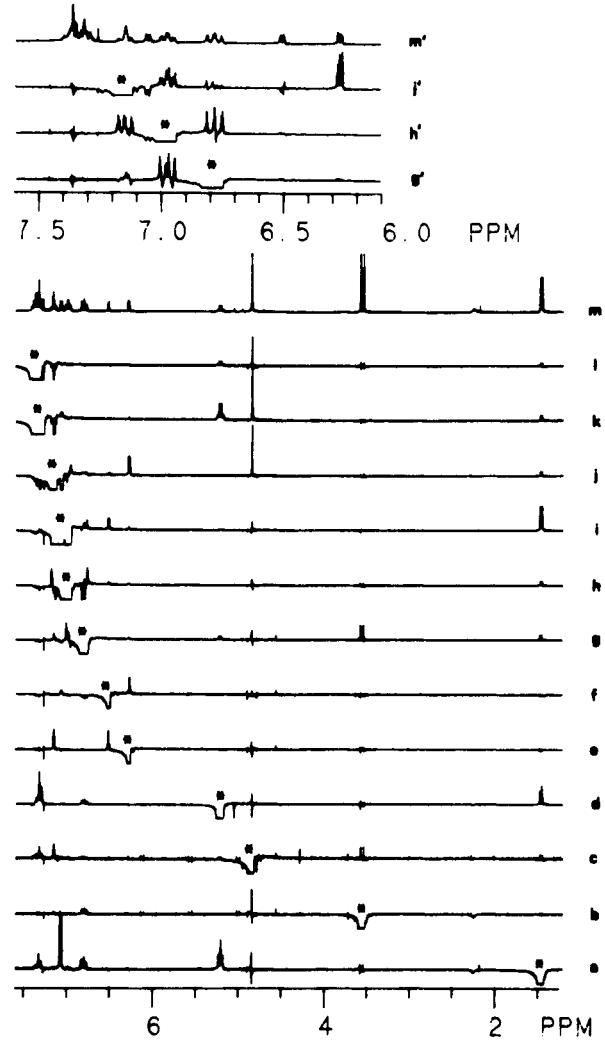


**Figure 2.** $^1$H nOed spectra of **4a** in $CD_3Cl$: (m, m′) reference spectrum; (a–l) difference spectra (×32) for irradiation at the indicated (*) frequency; (a) C*—Me; (b) P—OMe; (c) Cp; (d) C*H; (e) $H_4$; (f) $H_3$; (g,g′) $H_{ortho}$ of C*—Ph; (h, h′) $H_{meta}$; (i) CH=N; (j, j′) $H_5$ & $H_{para}$; (k) & (l) P—Ph; (g′, h′ j′ were obtained with a weaker decoupling power).

**Scheme III. Numbering Scheme and Major nOe Correlations**

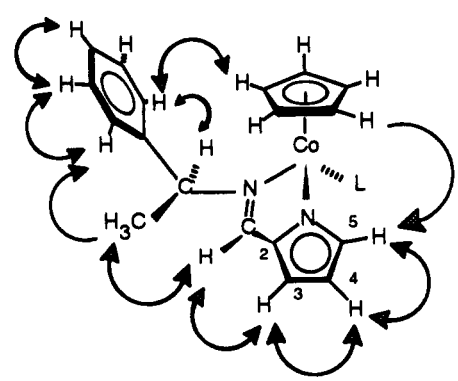


for 12 h resulted in no detectible Co epimerization; hence we infer a similar configurational stability for the isostructural intermediate **3a**. NMR spectra of **5a** and **3a** are very similar (cf. Tables I and II). A $^{31}$P singlet at 25.8 ppm for **5a** is characteristic for coordinated phosphine. $^1$H NMR shows distinct C*H, C*–Me, P–Me, and pyrrolyl resonances similar to those for **3a**. All carbon signals (cf. Table II) are well resolved and assigned clearly on the basis of $^1J$ $^1$H/$^{13}$C heterocorrelation spectra as for **3a**. The

Table II. $^{13}$C NMR for ($\eta^5$-Cp)Co(N-N*)(L) Complexes[a]

| no. | Cp | C(2) | C(3) | C(4) | C(5) | CH=N | C*H | POMe/PMe | Me | C*—Ph | P—Ph |
|---|---|---|---|---|---|---|---|---|---|---|---|
| **3a** | 88.69 | 142.39 | 120.61 | 116.37 | 144.21 | 159.11 | 69.42 | 57.87 (d, 11.6)[b]<br>57.33 (d, 12.0)[b] | 25.55 | 141.50[c]<br>132.51[d]<br>130.35[e]<br>130.19[e]<br>129.34[f] | 136.60 (d, 55.4)[g]<br>128.87[e]<br>128.74[e]<br>128.35[d]<br>126.28[f] |
| **3a**[h] | 89.83 | 144.49 | 121.88 | 117.05 | 145.27 | 162.20 | 71.10 | 57.30 (d, 13.2)[b]<br>57.12 (d, 13.2)[b] | 25.81 | 143.58[c]<br>133.70[d]<br>131.78[e]<br>131.63[e]<br>130.42[f] | 138.38 (d, 56.6)[g]<br>129.98[e]<br>129.84[e]<br>129.40[d]<br>127.71[f] |
| **4a** | 87.64 | 144.21 | 117.90 | 114.02 | 142.98 | 157.11 | 67.50 | 51.67 (d, 10.9)[b] | 25.29 | 141.81[c]<br>130.71[e]<br>130.57[e]<br>129.09[d]<br>126.94[f]<br>126.80[f] | 135.33 (d, 49.7)[g]<br>128.76[e]<br>127.56[d]<br>126.38[f] |
| **4b** | 87.81 | 144.16 | 117.27 | 113.72 | 143.00 | 157.81 | 68.05 | 50.99 (d, 11.9)[b] | 25.36 | 142.01[c]<br>129.96[e]<br>129.82[e]<br>129.47[d]<br>127.51[f]<br>127.37[f] | 135.60 (d, 50.4)[g]<br>128.79[e]<br>127.58[d]<br>126.39[f] |
| **5a** | 88.13 | 142.54 | 119.98 | 116.39 | 143.11 | 158.89 | 69.10 | 15.42 (d, 31.2)[i]<br>14.66 (d, 30.5)[i] | 25.75 | 141.58[c]<br>131.06[d]<br>129.78[e]<br>129.67[e]<br>129.08[f] | 132.24 (d, 47.3)[g]<br>128.97[e]<br>128.83[e]<br>128.01[d]<br>126.10[f] |

[a] $^{13}$C (75.47-MHz) NMR chemical shifts in ppm relative to solvent $CDCl_3$ = 77.00; d = doublet; $J$ values in Hz given in parentheses. [b] $^2J_{PC}$. [c] $C_{ipso}$. [d] $C_{para}$. [e] $C_{ortho}$. [f] $C_{meta}$. [g] $C_{ipso}$ ($^1J_{PC}$). [h] Solvent = methanol-$d_4$ (49.0 ppm). [i] $^1J_{PC}$.

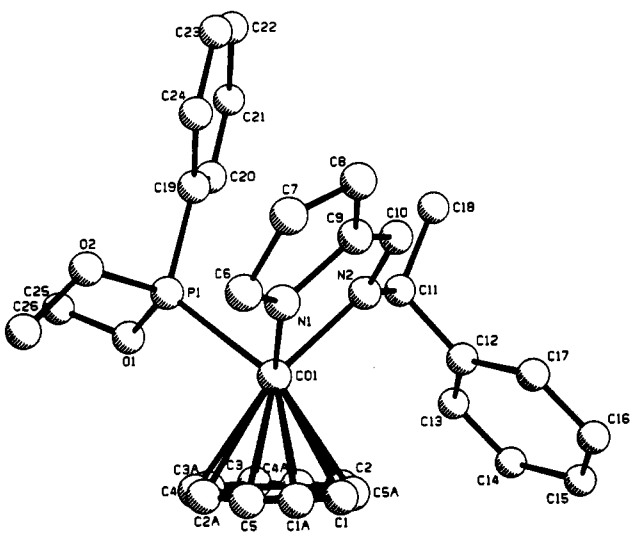


Figure 3. Molecular structure of **3a** ($I^-$ omitted for clarity).

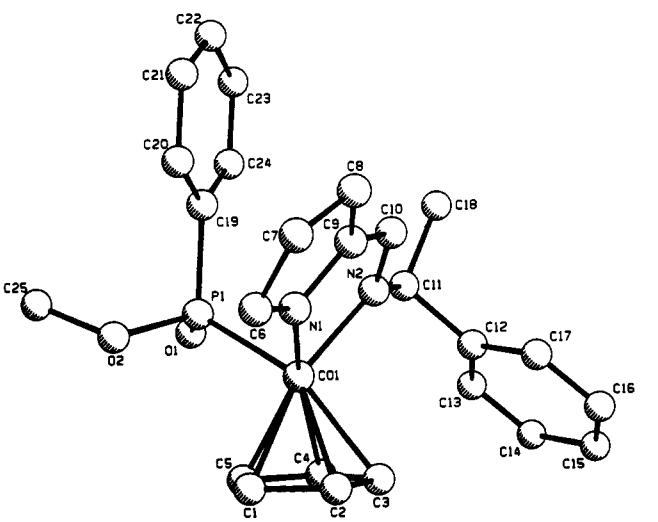


Figure 4. Molecular structure of **4a**·2$H_2O$ ($H_2O$ omitted for clarity).

isostructural complexes **3a** and **5a** adopt the similar solution conformation, as discussed below.

**Crystal Structure and Absolute Configuration of 3a, 4a·2$H_2O$, and 5a.** Absolute configurations of complexes **3a**, **4a**·2$H_2O$, and **5a** were assigned on the basis of crystallographic evidence. Crystallographic data are presented in Table IX. We have found that compounds in this series have a propensity to form twinned crystals, and such was the case for the specimen of **3a** selected for an X-ray crystallographic analysis. Nevertheless a well refined structure ($R_w$ = 0.041) with correct assignment of the absolute configuration consistent with the known absolute configuration at carbon ($S_C$) proved possible. The $\eta^5$-Cp group in **3a** is rotationally disordered, and refinement was carried out using a 55/45 occupancy model.

Refinement of the crystal structure of **4a** was complicated by the presence of disordered solvent in the unit cell. We were unable to grow a better quality crystal; however the overall structure and stereochemical assignments are consistent with spectroscopic parameters and the known absolute configuration of the internal reference $S_C$. The asymmetric unit contains two independent molecules (**4a**, **4a'**) each with one water molecule in close proximity as well as a more distant solvent cluster which was modeled as two water molecules with fractional occupancy. Thus, solid state samples of **4a** are formulated as dihydrates, **4a**·2$H_2O$ and **4a'**·2$H_2O$. The two crystallographically independent molecules have identical absolute configuration and differ only slightly in conformation (cf. Figure 5).

PLUTO representations of the structures of **3a**, **4a**·2$H_2O$, and **5a** are shown in Figure 3, 4, and 6, respectively. Coordinates, selected bond distances, and bond angles of **3a**, **4a**·2$H_2O$, **4a'**·2$H_2O$, and **5a** are given in Tables III–VII. All of these molecules are pseudooctahedral, three-legged piano-stools. The $\eta^5$-Cp moiety occupies three *facial* coordination sites with the P-donor and bidentate Schiff base (N–N*) ligands completing the coordination

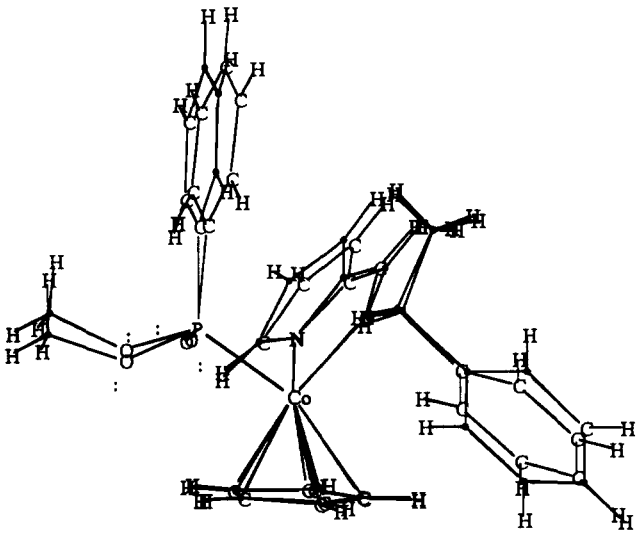

**Figure 5.** Structure comparison of **4a**·2$H_2O$ and **4a′**·2$H_2O$.

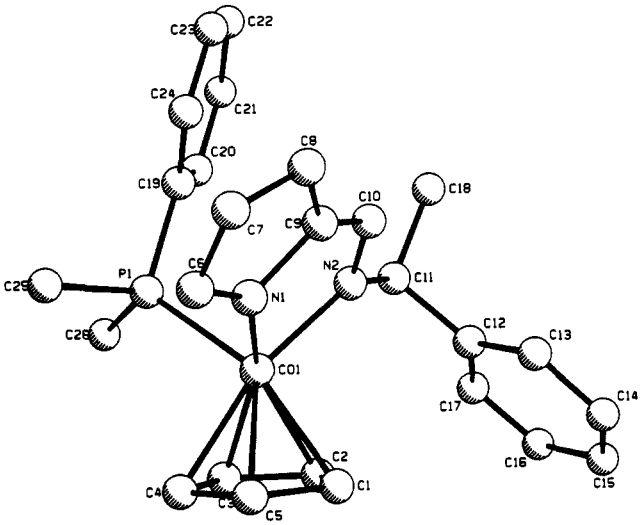


**Figure 6.** Molecular structure of **5a** ($I^-$ omitted for clarity).

sphere. Interligand bond angles (P–Co–N(1) (pyrrolyl), P–Co–N(2) (C*–N), N(1)–Co–N(2)) approximate 90°. The coordinated Schiff base is planar as a result of conjugation. All three molecules adopt a similar solid state conformation with C*–Ph syn and approximately edge-on and P–Ph anti to $\eta^5$-Cp. In each case the absolute configurations determined crystallographically were found to give the correct hand at the known $S_C$ center.

Consideration of these complexes as pseudotetrahedral cases with $\eta^5$-Cp effectively occupying one coordination site and use of the modified Cahn–Igold–Prelog rules[38-40] with the ligand priority series Cp > P-donor > N–C*H(Me)Ph > N–pyrrolyl fixes the absolute configuration of **3a**, **4a**·2$H_2O$, and **5a**, as $S_{Co}$. In the case of **4a**·2$H_2O$, the absolute configuration at P(O)(Ph)(OMe) with the priority series Co > OMe > O > Ph is $S_P$.

**Chiroptical Properties and Absolute Configuration of 4b.** The isomorphous CD spectra of **3a**, **4a**, and **5a** (Figure 7) are consistent with the same ($S_{Co}$) absolute configuration at cobalt as established from the X-ray crystal structure. Comparison of the CD spectra of the diastereomers **4a** and **4b** reveals a similar CD morphology *congruent with an identical absolute configuration at*

**Table III. Atomic Coordinates for ($S_{Co}$,$S_C$)-[($\eta^5$-Cp)Co(N–N*)(PPh(OMe)$_2$)]$^+I^-$, 3a**

| atom | x | y | z | B(eq)[a] (Å$^2$) | occupancy |
|---|---|---|---|---|---|
| I(1) | 0.60046(8) | 0.02239(6) | 0.2770(1) | 6.92(7) | |
| Co(I) | 0.5168(1) | 0.0934(1) | 0.7784(2) | 3.7(1) | |
| P(1) | 0.6279(3) | 0.1570(2) | 0.8736(4) | 3.7(2) | |
| O(1) | 0.6947(6) | 0.1035(5) | 0.9471(8) | 3.9(5) | |
| O(2) | 0.6938(7) | 0.2077(5) | 0.7917(9) | 5.1(5) | |
| N(1) | 0.4817(9) | 0.1798(6) | 0.687(1) | 4.5(7) | |
| N(2) | 0.4155(8) | 0.1277(6) | 0.8905(9) | 3.9(6) | |
| C(6) | 0.504(1) | 0.2178(9) | 0.581(1) | 5.8(4) | |
| C(7) | 0.444(1) | 0.2768(8) | 0.569(1) | 5.3(4) | |
| C(8) | 0.380(1) | 0.2762(8) | 0.661(1) | 4.7(4) | |
| C(9) | 0.400(1) | 0.2144(7) | 0.737(1) | 4.2(3) | |
| C(10) | 0.367(1) | 0.1828(8) | 0.849(1) | 4.1(4) | |
| C(11) | 0.386(1) | 0.0960(7) | 1.009(i) | 3.9(3) | |
| C(18) | 0.337(1) | 0.1476(9) | 1.099(1) | 5.7(4) | |
| C(25) | 0.779(1) | 0.125(1) | 1.008(1) | 6.4(5) | |
| C(26) | 0.754(1) | 0.185(1) | 0.692(2) | 7.3(5) | |
| C(19) | 0.5905(6) | 0.2248(4) | 0.9815(7) | 3(1) | |
| C(20) | 0.5874(6) | 0.2059(4) | 1.1060(8) | 4(1) | |
| C(21) | 0.5601(6) | 0.2585(5) | 1.1933(6) | 6(1) | |
| C(22) | 0.5359(6) | 0.3301(5) | 1.1561(8) | 5(1) | |
| C(23) | 0.5390(6) | 0.3490(4) | 1.0317(9) | 6(1) | |
| C(24) | 0.5663(6) | 0.2963(5) | 0.9444(6) | 4(1) | |
| C(12) | 0.3267(6) | 0.0259(5) | 0.9968(8) | 4(2) | |
| C(13) | 0.3501(5) | –0.0362(6) | 1.0670(7) | 6(2) | |
| C(14) | 0.2943(7) | –0.1003(5) | 1.0571(8) | 6(2) | |
| C(15) | 0.2152(6) | –0.1024(4) | 0.9771(8) | 6(2) | |
| C(16) | 0.1917(5) | –0.0403(6) | 0.9069(7) | 6(2) | |
| C(17) | 0.2475(7) | 0.0239(5) | 0.9168(7) | 5(2) | |
| C(1) | 0.459(1) | 0.007(1) | 0.673(2) | 3.6(2) | 0.550 |
| C(2) | 0.470(1) | –0.020(1) | 0.793(2) | 3.6(2) | 0.550 |
| C(3) | 0.569(2) | –0.016(1) | 0.824(1) | 3.6(2) | 0.550 |
| C(4) | 0.6187(8) | 0.014(1) | 0.723(2) | 3.6(2) | 0.550 |
| C(5) | 0.551(2) | 0.028(1) | 0.630(1) | 3.6(2) | 0.550 |
| C(1A) | 0.500(2) | 0.026(2) | 0.621(2) | 4.0(3) | 0.450 |
| C(2A) | 0.598(2) | 0.031(2) | 0.650(2) | 4.0(3) | 0.450 |
| C(3A) | 0.612(1) | 0.002(2) | 0.768(2) | 4.0(3) | 0.450 |
| C(4A) | 0.521(2) | –0.020(1) | 0.813(2) | 4.0(3) | 0.450 |
| C(5A) | 0.452(1) | –0.006(2) | 0.722(3) | 4.0(3) | 0.450 |

[a] $B_{eq} = 8(\pi^2/3)\sum_{i=1}^{3}\sum_{j=1}^{3}U_{ij}a_i^*a_j^*\vec{a}_i\vec{a}_j$.

*cobalt* ($S_{Co}$). The absolute configuration at phosphorus in **4b** must be $R_P$ since **4a** and **4b** are the *only* products observed when ion-pair **3a** collapses with retention at cobalt in solution.

**Stereochemistry of the Arbuzov Dealkylation 3 → 4.** There can be little question[4] that simple halide substitution to give a cationic intermediate is the first step in the transition metal Arbuzov reaction. Subsequent nucleophilic attack at carbon on prochiral $P(OR)_2$ for the complexes examined in this study is diastereoselective, evolving under the influence of the chiral cobalt center. If we accept that configurationally stable **5a** is a good model for **3a**, comparison of the absolute stereochemistry of ($S_{Co}$)-**3a** and ($S_{Co}$)-**4a,b** establishes that Arbuzov dealkylation proceeds exclusively with retention at the metal center, as required by Scheme IV. That the chiral induction in this reaction is much less than that found for ligand spheres *containing the hydrogen bonding* (*S*)-$Ph_2PN(H)C^*H(Me)$-Ph (PNH*) as a ligand[26,31] is consistent with the importance of noncovalent P=O···HN hydrogen bonding in the chiral induction of Arbuzov dealkylation.

**Solution Conformation.** Proton nuclear Overhauser effect difference (nOed) spectroscopy[26-28,32,36,41-44] was used to study the solution conformation of **3a**, **4a**, and **5a**. Comprehensive analysis showed that all three complexes adopt a similar conformation both in solution and in the

(38) Cahn, R. S.; Ingold, C.; Prelog, V. *Angew. Chem., Int. Ed. Engl.* **1966**, *5*, 385–415.
(39) Stanley, K.; Baird, M. C. *J. Am. Chem. Soc.* **1975**, *97*, 6598–9.
(40) Sloan, T. E. *Top. Stereochem.* **1981**, *12*, 1–36.
(41) Sanders, J. K. M.; Mersh, J. D. *Prog. Nucl. Magn. Reson. Spectrosc.* **1983**, *15*, 353–400.
(42) Jablonski, C. R.; Zhou, Z. *Can. J. Chem.* **1992**, *70*, 2544–51.

**Table IV. Atomic Coordinates for ($S_{Co}$,$S_P$,$S_C$)-($\eta^5$-Cp)Co(N-N*)(P(O)(Ph)(OMe)), 4a·2H$_2$O, 4a′·2H$_2$O**

| atom | x | y | z | B(eq)[a] (Å$^2$) | occupancy |
|---|---|---|---|---|---|
| Co(1) | −0.0251(2) | 0.0716(1) | −0.1302(3) | 4.0(2) | |
| Co(1′) | 0.0770(2) | 0.3466(1) | 0.4561(3) | 4.0(2) | |
| P(1) | 0.1035(3) | 0.0749(2) | −0.1721(5) | 4.6(3) | |
| P(1′) | −0.0493(3) | 0.3603(2) | 0.4069(5) | 4.9(4) | |
| O(1) | 0.1524(6) | 0.0398(4) | −0.114(1) | 5.5(3) | |
| O(1′) | −0.0825(7) | 0.3973(4) | 0.488(1) | 6.7(4) | |
| O(2) | 0.1111(7) | 0.0787(4) | −0.342(1) | 6.1(3) | |
| O(2′) | −0.0470(7) | 0.3690(4) | 0.238(1) | 5.6(3) | |
| O(3) | 0.1251(6) | −0.0214(3) | 0.084(1) | 5.4(3) | |
| O(4) | 0.292(1) | −0.0011(6) | −0.171(2) | 16.4(7) | |
| O(5) | −0.686(2) | 0.083(1) | −0.719(3) | 11(1) | 0.500 |
| O(6) | −0.613(4) | 0.082(3) | −0.768(8) | 15(1) | 0.300 |
| O(7) | −0.564(2) | 0.073(2) | −0.791(6) | 15(1) | 0.400 |
| O(8) | −0.596(3) | 0.042(1) | −0.941(5) | 15(1) | 0.400 |
| O(9) | −0.671(3) | 0.024(1) | −0.887(5) | 16(1) | 0.400 |
| N(1) | −0.0470(8) | 0.1275(4) | −0.190(2) | 4.2(4) | |
| N(1′) | 0.0730(8) | 0.2923(4) | 0.377(2) | 5.1(4) | |
| N(2) | −0.0097(7) | 0.0975(4) | 0.056(1) | 3.3(3) | |
| N(2′) | 0.0437(7) | 0.3170(4) | 0.625(1) | 3.1(3) | |
| C(6) | −0.070(1) | 0.1491(7) | −0.314(2) | 6.6(5) | |
| C(6′) | 0.086(1) | 0.2753(6) | 0.246(2) | 5.3(5) | |
| C(7) | −0.085(1) | 0.1891(6) | −0.263(2) | 5.7(5) | |
| C(7′) | 0.075(1) | 0.2324(6) | 0.261(2) | 4.8(5) | |
| C(8) | −0.070(1) | 0.1942(6) | −0.123(2) | 6.4(5) | |
| C(8′) | 0.056(1) | 0.2232(6) | 0.401(2) | 6.2(5) | |
| C(9) | −0.048(1) | 0.1538(6) | −0.078(2) | 5.0(5) | |
| C(9′) | 0.053(1) | 0.2628(6) | 0.469(2) | 4.3(5) | |
| C(10) | −0.025(1) | 0.1381(5) | 0.053(2) | 4.1(4) | |
| C(10′) | 0.036(1) | 0.2779(6) | 0.603(2) | 4.4(5) | |
| C(11) | 0.019(1) | 0.0766(6) | 0.183(2) | 4.8(5) | |
| C(11′) | 0.026(1) | 0.3373(5) | 0.771(2) | 4.1(5) | |
| C(18) | 0.052(1) | 0.1054(6) | 0.300(2) | 7.1(6) | |
| C(18′) | −0.027(1) | 0.3105(6) | 0.866(2) | 6.9(5) | |
| C(25) | 0.190(1) | 0.0807(7) | −0.405(2) | 9.9(7) | |
| C(25′) | −0.118(1) | 0.3835(7) | 0.170(2) | 8.6(6) | |
| C(1) | −0.0748(9) | 0.0404(4) | −0.302(1) | 7.3(4) | |
| C(2) | −0.1370(6) | 0.0497(3) | −0.207(1) | 5.9(4) | |
| C(3) | −0.1197(7) | 0.0307(4) | −0.077(1) | 5.9(4) | |
| C(4) | −0.0469(7) | 0.0096(3) | −0.091(i) | 5.7(4) | |
| C(5) | −0.0192(6) | 0.0156(4) | −0.231(2) | 6.9(4) | |
| C(1′) | 0.1403(8) | 0.3782(4) | 0.304(1) | 6.6(4) | |
| C(2′) | 0.1964(6) | 0.3574(3) | 0.389(2) | 6.0(4) | |
| C(3′) | 0.1880(6) | 0.3717(3) | 0.529(1) | 5.2(4) | |
| C(4′) | 0.1268(7) | 0.4013(3) | 0.530(1) | 5.8(4) | |
| C(5′) | 0.0973(5) | 0.4053(3) | 0.391(1) | 4.8(4) | |
| C(19) | 0.1508(7) | 0.1215(3) | −0.108(2) | 4.7(3) | |
| C(20) | 0.1400(5) | 0.1584(5) | −0.183(1) | 6.5(3) | |
| C(21) | 0.1754(8) | 0.1948(3) | −0.134(1) | 9.1(3) | |
| C(22) | 0.2215(6) | 0.1943(3) | −0.010(2) | 6.6(3) | |
| C(23) | 0.2324(5) | 0.1574(5) | 0.065(1) | 9.1(3) | |
| C(24) | 0.1970(8) | 0.1210(3) | 0.016(1) | 6.2(3) | |
| C(19′) | −0.1184(6) | 0.3175(3) | 0.424(2) | 4.4(3) | |
| C(20′) | −0.1744(8) | 0.3174(3) | 0.535(1) | 6.7(3) | |
| C(21′) | −0.2264(6) | 0.2840(5) | 0.551(1) | 8.7(3) | |
| C(22′) | −0.2224(7) | 0.2506(3) | 0.457(2) | 7.7(3) | |
| C(23′) | −0.1663(9) | 0.2507(3) | 0.347(1) | 9.0(3) | |
| C(24′) | −0.1144(6) | 0.2842(5) | 0.330(1) | 6.7(3) | |
| C(12) | −0.0481(6) | 0.0506(4) | 0.254(1) | 3.3(2) | |
| C(13) | −0.0304(5) | 0.0111(4) | 0.304(1) | 4.6(2) | |
| C(14) | −0.0896(8) | −0.0123(2) | 0.371(1) | 5.1(2) | |
| C(15) | −0.1664(6) | 0.0039(4) | 0.389(1) | 5.6(2) | |
| C(16) | −0.1841(5) | 0.0435(4) | 0.338(1) | 5.6(2) | |
| C(17) | −0.1250(8) | 0.0668(3) | 0.271(1) | 4.1(2) | |
| C(12′) | 0.1054(5) | 0.3472(4) | 0.842(1) | 4.7(3) | |
| C(13′) | 0.1212(6) | 0.3876(4) | 0.885(1) | 5.2(3) | |
| C(14′) | 0.1935(8) | 0.3971(3) | 0.952(1) | 5.7(3) | |
| C(15′) | 0.2500(5) | 0.3661(4) | 0.976(1) | 6.0(3) | |
| C(16′) | 0.2343(6) | 0.3256(3) | 0.932(1) | 4.7(3) | |
| C(17′) | 0.1620(7) | 0.3162(3) | 0.865(1) | 4.7(3) | |

[a] $B_{eq} = 8(\pi^2/3)\sum_{i=1}^{3}\sum_{j=1}^{3}U_{ij}a_i^*a_j^*\vec{a}_i\vec{a}_j$.

**Table V. Atomic Coordinates for ($S_{Co}$,$S_C$)-[($\eta^5$-Cp)Co(N-N*)(PPhMe$_2$)]$^+$I$^-$, 5a**

| atom | x | y | z | B(eq)[a] (Å$^2$) |
|---|---|---|---|---|
| I(1) | 0.3991(1) | 0.4840(1) | 0.7197(2) | 9.1(1) |
| Co(1) | 0.9805(2) | 0.0986(1) | 0.7569(3) | 3.0(1) |
| P(1) | 0.8617(4) | 0.1646(3) | 0.6603(5) | 4.1(3) |
| N(1) | 1.025(1) | 0.1851(8) | 0.849(1) | 4.1(4) |
| N(2) | 1.087(1) | 0.1296(7) | 0.648(1) | 2.6(3) |
| C(6) | 1.001(2) | 0.226(1) | 0.953(2) | 7.1(6) |
| C(7) | 1.067(2) | 0.284(1) | 0.962(2) | 5.7(6) |
| C(8) | 1.131(1) | 0.283(1) | 0.867(2) | 4.8(5) |
| C(9) | 1.109(1) | 0.221(1) | 0.793(2) | 4.6(5) |
| C(10) | 1.138(1) | 0.188(1) | 0.683(2) | 3.7(5) |
| C(11) | 1.112(1) | 0.0946(9) | 0.524(2) | 3.5(4) |
| C(18) | 1.164(1) | 0.147(1) | 0.430(2) | 5.6(5) |
| C(25) | 0.787(1) | 0.215(1) | 0.771(2) | 7.2(6) |
| C(26) | 0.767(1) | 0.113(1) | 0.574(2) | 5.1(5) |
| C(1) | 1.0471(6) | 0.0076(7) | 0.845(1) | 5.2(5) |
| C(2) | 1.0008(8) | −0.0135(5) | 0.734(1) | 5.8(5) |
| C(3) | 0.8982(7) | 0.0028(6) | 0.743(1) | 4.9(4) |
| C(4) | 0.8811(7) | 0.0341(6) | 0.860(1) | 5.9(5) |
| C(5) | 0.973(1) | 0.0371(6) | 0.9231(8) | 5.8(5) |
| C(12) | 1.1768(7) | 0.0248(5) | 0.540(1) | 2.4(4) |
| C(13) | 1.2589(8) | 0.0236(6) | 0.620(1) | 4.7(5) |
| C(14) | 1.3162(6) | −0.0409(7) | 0.6327(8) | 5.1(5) |
| C(15) | 1.2914(8) | −0.1043(5) | 0.565(1) | 6.3(6) |
| C(16) | 1.2093(9) | −0.1032(5) | 0.484(1) | 5.5(5) |
| C(17) | 1.1520(6) | −0.0386(7) | 0.4721(9) | 4.8(5) |
| C(19) | 0.9092(8) | 0.2302(6) | 0.550(1) | 3.2(4) |
| C(20) | 0.8999(7) | 0.2126(5) | 0.424(1) | 4.1(4) |
| C(21) | 0.9357(8) | 0.2617(7) | 0.3347(8) | 5.9(6) |
| C(22) | 0.9809(7) | 0.3284(6) | 0.370(1) | 5.8(6) |
| C(23) | 0.9902(7) | 0.3460(5) | 0.496(1) | 5.1(5) |
| C(24) | 0.9543(8) | 0.2969(6) | 0.5855(8) | 4.6(5) |

[a] $B_{eq} = 8(\pi^2/3)\sum_{i=1}^{3}\sum_{j=1}^{3}U_{ij}a_i^*a_j^*\vec{a}_i\vec{a}_j$.

**Table VI. Selected Bond Distances (Å) for 3a, 4a·2H$_2$O, 4a′·2H$_2$O, and 5a**

| | 3a | 4a·2H$_2$O | 4a′·2H$_2$O | 5a |
|---|---|---|---|---|
| Co(1)–P(1) | 2.175(5) | 2.186(5) | 2.203(6) | 2.236(6) |
| Co(1)–N(1) | 1.92(1) | 1.93(1) | 1.19(1) | 1.94(1) |
| Co(1)–N(2) | 1.95(1) | 1.95(1) | 1.94(1) | 1.93(1) |
| Co(1)–C(1) | 2.09(2) | 2.08(1) | 2.05(1) | 2.09(1) |
| Co(1)–C(2) | 2.16(2) | 2.12(1) | 2.12(1) | 2.05(1) |
| Co(1)–C(3) | 2.16(2) | 2.12(1) | 2.13(1) | 2.05(1) |
| Co(1)–C(4) | 2.09(2) | 2.07(1) | 2.07(1) | 2.08(1) |
| Co(1)–C(5) | 2.05(2) | 2.04(1) | 2.02(1) | 2.11(1) |
| Co(1)–C(1A) | 2.12(2) | | | |
| Co(1)–C(2A) | 2.12(2) | | | |
| Co(1)–C(3A) | 2.10(3) | | | |
| Co(1)–C(4A) | 2.09(3) | | | |
| Co(1)–C(5A) | 2.10(3) | | | |
| P(1)–O(1) | 1.556(9) | 1.50(1) | 1.52(1) | |
| P(1)–O(2) | 1.57(1) | 1.60(1) | 1.61(1) | |
| P(1)–C(19) | 1.772(9) | 1.80(1) | 1.81(1) | 1.79(1) |
| N(1)–C(6) | 1.37(2) | 1.41(2) | 1.37(2) | 1.37(3) |
| N(1)–C(9) | 1.40(2) | 1.35(2) | 1.33(2) | 1.43(2) |
| N(2)–C(10) | 1.28(2) | 1.33(2) | 1.29(2) | 1.30(2) |
| N(2)–C(11) | 1.47(2) | 1.45(2) | 1.54(2) | 1.51(2) |
| C(6)–C(7) | 1.35(2) | 1.40(3) | 1.41(3) | 1.36(3) |
| C(7)–C(8) | 1.34(2) | 1.35(3) | 1.38(3) | 1.33(3) |
| C(8)–C(9) | 1.42(2) | 1.42(3) | 1.43(3) | 1.41(3) |
| C(9)–C(10) | 1.42(2) | 1.39(2) | 1.38(3) | 1.39(3) |

solid state. nOed spectra for **3a** showed that P—Ph and C*—Me are distal while C*—Ph and P—OMe are proximal to $\eta^5$-Cp. Irradiation of C*—Me at 1.52 ppm (Figure 1b) shows strong correlation to CH=N at 7.52 ppm (13.7%), $H_{ortho}$ of C*—Ph (2.7%), and C*H (10.0%), indicating that the C*—Me bond eclipses CH=N, as shown in Figure 3. This was confirmed by the lack of enhancement of the CH=N resonance and small enhancements of Cp (0.6%), $H_{ortho}$ of C*—Ph (1.3%), and C*—Me (1.4%) (Figure 1e), respectively, on irradiation of the C*H resonance at 4.76 ppm. The solid state, edge-on, syn C*—Ph/$\eta^5$-Cp, considered to be the low energy conformation in similar

(43) Faller, J. W.; Crabtree, R. H.; Habib, A. *Organometallics* **1985**, *4*, 929–35.
(44) Crabtree, R. H.; Parnell, C. P. *Organometallics* **1984**, *3*, 1727–31.

**Table VII. Selected Bond Angles (deg) for 3a, 4a·2H$_2$O, 4a′·2H$_2$O, and 5a**

| | 3a | 4a·2H$_2$O | 4a′·2H$_2$O | 5a |
|---|---|---|---|---|
| P(1)–Co(1)–N(2) | 89.7(4) | 95.1(4) | 94.0(5) | 91.5(4) |
| P(1)–Co(1)–N(2) | 92.2(3) | 90.6(4) | 89.8(4) | 94.8(4) |
| N(1)–Co(1)–N(2) | 83.4(5) | 83.3(6) | 81.5(6) | 81.8(6) |
| Co(1)–P(1)–O(1) | 109.3(4) | 115.7(5) | 113.6(5) | 110.5(7)[a] |
| Co(1)–P(1)–O(2) | 116.5(4) | 105.0(5) | 102.6(5) | 117.5(6)[b] |
| Co(1)–P(1)–C(19) | 118.4(3) | 114.2(5) | 115.9(4) | 114.2(4) |
| O(1)–P(1)–O(2) | 108.1(5) | 112.2(7) | 111.4(7) | 102.1(8)[c] |
| O(1)–P(1)–C(19) | 105.2(5) | 105.8(6) | 108.9(7) | 107.8(7)[d] |
| O(2)–P(1)–C(19) | 98.0(5) | 103.3(7) | 103.8(7) | 103.7(7)[e] |
| Co(1)–N(1)–C(6) | 142(1) | 139(1) | 136(1) | 141(1) |
| Co(1)–N(1)–C(9) | 111.3(8) | 111(1) | 115(1) | 112(1) |
| Co(1)–N(2)–C(10) | 113.4(9) | 112(1) | 113(1) | 116(1) |
| Co(1)–N(2)–C(11) | 128.4(9) | 125(1) | 124.6(9) | 125(2) |
| C(10)–N(2)–C(11) | 118(1) | 122(1) | 123(1) | 119(1) |
| N(1)–C(6)–C(7) | 110(1) | 103(2) | 106(2) | 109(2) |
| N(1)–C(9)–C(8) | 106(1) | 111(2) | 110(2) | 106(2) |
| N(1)–C(9)–C(10) | 115(1) | 117(2) | 113(2) | 113(2) |
| C(6)–C(7)–C(8) | 108(1) | 114(2) | 110(2) | 111(2) |
| C(7)–C(8)–C(9) | 108(1) | 103(2) | 104(2) | 108(2) |
| C(8)–C(9)–C(10) | 139(1) | 132(2) | 137(2) | 141(2) |
| N(2)–C(10)–C(9) | 117(1) | 115(2) | 118(2) | 117(2) |
| N(2)–C(11)–C(12) | 114(1) | 111(1) | 108(1) | 111(1) |
| N(2)–C(11)–C(18) | 117(1) | 115(1) | 112(1) | 115(1) |

[a] Co(1)–P(1)–C(25). [b] Co(1)–P(1)–C(26). [c] C(25)–P(1)–C(26). [d] C(25)–P(1)–C(19). [e] C(26)–P(1)–C(19).

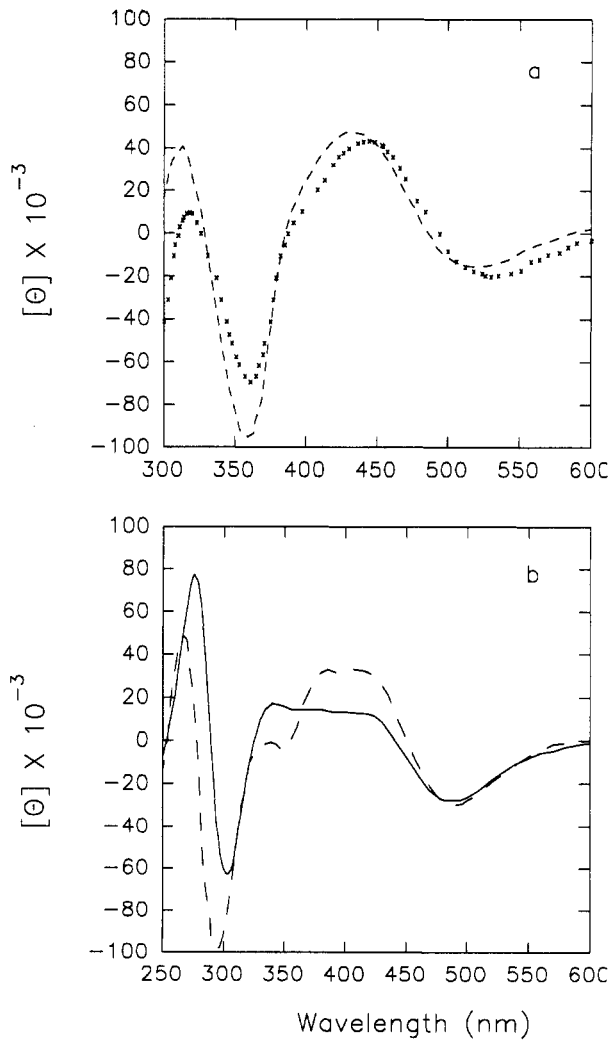


**Figure 7.** Circular dichroism (CD) spectra of (a) **3a** (- - -) and **5a** (×) and (b) **4a** (– –) and **4b** (—).

cyclopentadienyl piano-stool complexes,[32,45] persists in solution as indicated by irradiation of the Cp resonance at 5.35 ppm (Figure 1f) which gives an 0.8% enhancement of $H_{ortho}$ of C*—Ph and a 1.5% enhancement of $H_{meta}$ and $H_{para}$ of C*—Ph, respectively. No correlation between Cp and P—Ph was observed when the Cp (Figure 1f) and P—Ph (Figure 1k) resonances were irradiated, indicating that P—Ph is distal with respect to Cp. Irradiation of P—OMe at 3.82 and 4.05 ppm gave small, positive enhancements (0.5% and 0.4%) of Cp (Figure 1c,d), respectively. Irradiation of Cp showed 1.7% and 1.4% enhancement to the diastereotopic P(OMe)$_2$ groups (Figure 1f). Similar nOed patterns were observed for **4a** and **5a**, establishing that the solid state conformation is retained in solution for all three complexes.

**Kinetic Studies.** The isolation of the intermediate **3a** enabled us not only to investigate the chiral induction from Co* → P but also to directly measure the kinetics for the Arbuzov dealkylation step. NMR studies showed that two parallel dealkylation reactions occur as shown in Scheme IV when **3a** is dissolved. Kinetic data were analyzed by fitting integrated $^1$H NMR time profiles for the appearance of **4a** and **4b** to the first order expression $A_i = A_{i\infty}(1 - \exp(-k_i t))$ using an iterative, nonlinear least squares procedure. Good fits over >2 half-lives were obtained in methylene chloride and acetone. The reaction is significantly slower in acetonitrile but remains first order (0.2 half-life) and does not proceed to a significant extent under similar conditions in methanol. A representative set of experimental and calculated data for the disappearance of **3a** and appearance of **4a** and **4b** is shown in Figure 8.

A first order rate law follows from a kinetic model which assumes pre-equilibrium ion-pair formation, $\mathbf{3a}^+ + I^- \leftrightarrow \mathbf{3a}^+,I^-$, with $\alpha \ll 1$ (where $\alpha$ is the degree of dissociation, $\alpha = [\mathbf{3a}^+]/C(\mathbf{3a})$),[46] and a rate determining conversion of the ion pair into products. Chiral induction in Scheme IV depends on the ratio $k_1/k_2$, leading to ($S_{Co}$,$S_P$,$S_C$)-**4a** and ($S_{Co}$,$R_P$,$S_C$)-**4b**, respectively. The first order rate constants $k_1$ and $k_2$ for the reactions **3a** → **4a** and **3a** → **4b**, respectively, obtained as described above, are summarized in Table VIII. Good agreement was obtained between the sum $k_1 + k_2$ and independently determined experimental values for the rate constant $k_t$ for the first order consumption of **3a**, verifying the rate law $-d[\mathbf{3a}]/dt = k_t[\mathbf{3a}] = (k_1 + k_2)[\mathbf{3a}]$ appropriate for product formation via two parallel first order reactions.

Several qualitative conclusions can be drawn from the kinetic data summarized in Table VIII: (i) $k_1$ and $k_2$ are sensitive to solvent with $k$(methylene chloride) ≈ $k$(acetone) > $k$(acetonitrile) ≫ $k$(methanol). As is generally expected for cation/anion reactions involving charge destruction, reaction rate is inversely related to solvent dielectric.[47] Parker's critical analysis[48] reconciles the observation that reactions of the charge type shown in Scheme IV are much slower in protonic vs aprotic dipolar solvents in terms of hydrogen bonding of the anion, $X^-$. Protonic solvents are strong hydrogen bond donors and therefore solvate anions as reflected by the free energy of transfer of ions from a reference solvent,[49] $\Delta G_{tr}$. With DMF as a reference, $\Delta G_{tr}(I^-)$ becomes less favorable along the solvent series methanol ($\Delta G_{tr}(I^-)$ = −10 kJ/mol) >

(45) Bernal, I.; Reisner, G. M.; Brunner, H.; Riepl, G. *J. Organomet. Chem.* **1985**, *284*, 115–28.
(46) Moore, J. W.; Pearson, R. G. *Kinetics and Mechanism*; John Wiley and Sons: New York, 1981.
(47) Amis, E. S. *Solvent Effects on Reaction Rates and Mechanisms*; Academic Press: New York, 1966.
(48) Parker, A. J. *Chem. Rev.* **1969**, *69*, 1–32.
(49) Parker, A. J.; Mayer, U.; Schmid, R.; Gutmann, V. *J. Org. Chem.* **1978**, *43*, 1843–54.

**Scheme IV**

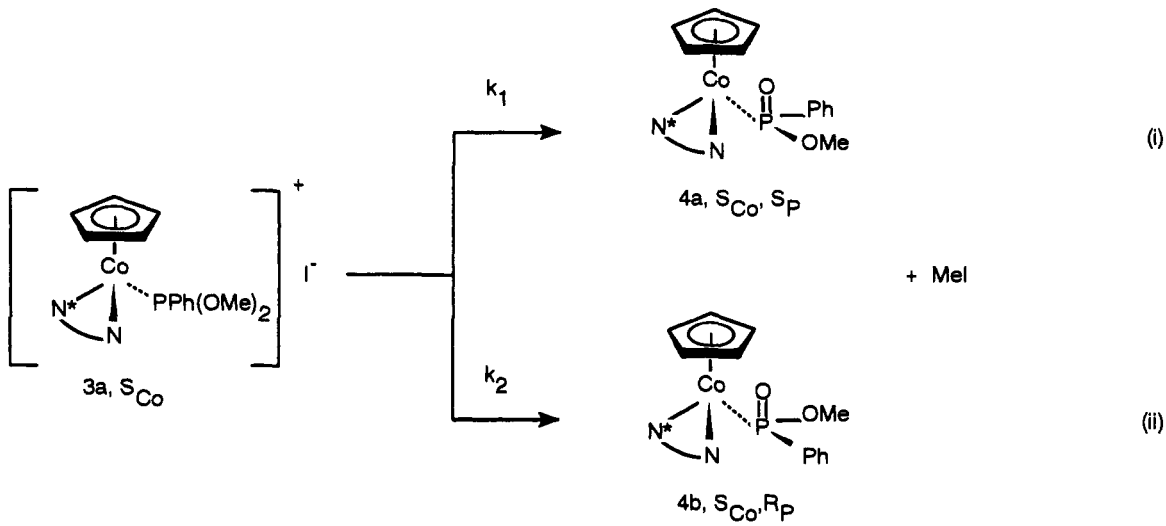


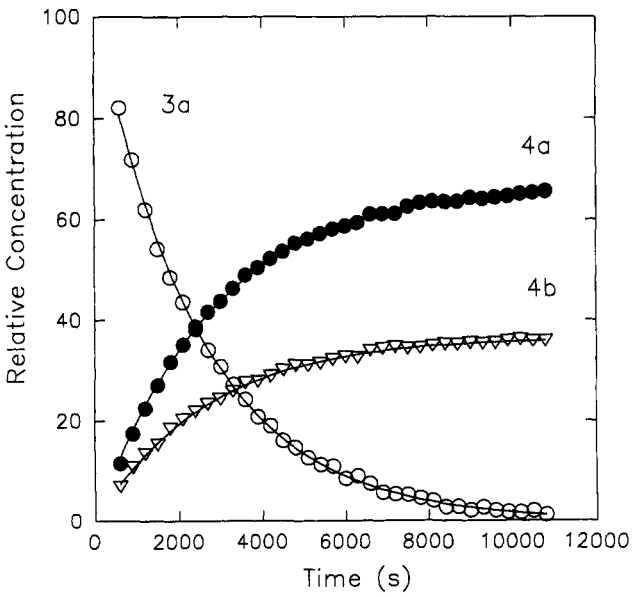


**Figure 8.** Representative integrated concentration vs time profile of experimental and fitted data for Scheme IV, run 7 in Table VIII.

acetonitrile ($\Delta G_{tr}(I^-)$ = −4 kJ/mol) > acetone ($\Delta G_{tr}(I^-)$ = +8 kJ/mol). Assuming that changes in anion solvation dominate, $\Delta G_{tr}(I^-)$ reflects the order of reaction rates measured for Scheme IV. Presumably, the Arbuzov dealkylation of Scheme IV, which requires collapse of the ion pair via $S_N2$ attack of iodide on carbon, does not proceed in methanol since $I^-$ is very strongly solvated compared to the case of aprotic dipolar solvents. In acetone, anion solvation is poor since hydrogen bonding cannot occur, the degree of dissociation $\alpha$ is very low, and $k_{obs}$ is large and insensitive to added halide. (ii) The kinetic product ratio $k_1/k_2$ is relatively independent of solvent, as expected if $\Delta G_{tr}(I^-)$ dominates the solvent effect on the reaction rate. $k_1/k_2$ = 1.6 in methylene chloride ($\epsilon$ = 8.9), 1.8 in acetone ($\epsilon$ = 20.7), and 1.5 in acetonitrile ($\epsilon$ = 37.5) so that dealkylation favors the formation of $(S_{Co},S_P,S_C)$-**4a** with ca. 25(3)% de. We conclude that the reaction proceeds via collapse of a tight-ion pair in aprotic solvent.

## Experimental Section

**Reagents and Methods.** All manipulations were performed under a dry nitrogen atmosphere using standard Schlenk techniques. Nitrogen gas was purified by passing through a series of columns containing DEOX (Alpha) catalyst heated to 120 °C, granular $P_4O_{10}$, and finally activated 3-A molecular sieves. Benzene, hexane, and pentane solvents were distilled under nitrogen from blue solutions of sodium benzophenone ketyl. Methylene chloride was distilled under nitrogen from $P_4O_{10}$. $PPh(OMe)_2$ and $PPhMe_2$ were purchased from Aldrich and Strem, respectively, and used as received. Chromatographic separations were carried out using a Chromatotron (Harrison Associates) with 4-mm-thick silica $gel_{60}PF_{254}$ (Merck) absorbent. Thin-layer chromatographic separations were performed on analytical thin-layer precoated TLC plates (silica gel F-254, Merck). Elemental analyses were performed by Canadian Microanalytical Services (Delta, BC). Melting points were determined in sealed capillaries and are uncorrected. NMR spectra were recorded on a GE 300-NB Fourier transform spectrometer operating at a proton frequency of 300.12 MHz. Optical rotation measurements were determined in methylene chloride (ca. 1 mg/mL) in a 1-cm path length cell by using a Perkin-Elmer Model 141 polarimeter. Circular dichroism (CD) spectra were determined in methylene chloride (ca. 1 mg/mL) on a Jasco J 40 A apparatus using a 0.1-cm path length cell. $\eta^5$-CpCo(CO)$(I)_2$ (**1**)[50,51] and $\eta^5$-CpCo(N–N*)(I) (**2a,b**)[32] were prepared using the established procedures.

Proton nOed spectra were determined under steady state conditions on the GE 300-NB instrument. Data were collected using interleaved experiments of 16 or 32 transients cycled 12–16 times through the list of decoupling frequencies. In each experiment the decoupler was gated on in continuous wave (CW) mode for 2–6 s with sufficient attenuation to give an approximate 70–90% reduction in intensity of the irradiated peak. A 60-s delay preceded each frequency change. A set of four equilibrating scans was employed to equilibrate the spins prior to data acquisition. No relaxation delay was applied between successive scans of a given decoupling frequency. Difference spectra were obtained on 16K or zero-filled 32K data tables which had been digitally filtered with a 0.1-Hz exponential or Gaussian line broadening function. Quantitative data were obtained by integration.

**Crystal Structure Determinations (General).** Crystal data were collected at ambient temperature on a Rigaku AFC6S diffractometer using the $\omega$-2$\theta$ scan technique to a maximum 2$\theta$ value of 45.1° (**3a**), 100.1° (**4a**·$2H_2O$), and 120.2° (**5a**), respectively. Structures were solved by direct methods[52] using the Molecular Structure Corp. TEXSAN software. The selected crystal for **3a** proved to be twinned, showing broad, unsymmetrical peaks which

(50) King, R. B. *Inorg. Chem.* **1966**, *5*, 82–7.
(51) Frith, S. A.; Spencer, J. L. *Inorg. Synth.* **1984**, *23*, 15–21.
(52) Gilmore, C. J. *J. Appl. Crystallogr.* **1984**, *17*, 42–6.
(53) Walker, N.; Stuart, D. *Acta Crystallogr., Sect. A* **1983**, *A39*, 158–66.

**Table VIII. Kinetic Data for Reaction 3a → 4a + 4b**

| no. | solvent | $\epsilon$ | $C_0$ (3a) (mol·L$^{-1}$) | $C$ (LiI) (mol·L$^{-1}$) | $T$ (K) | $10^{-4}k_1$ (s$^{-1}$) | $10^{-4}k_2$ (s$^{-1}$) |
|---|---|---|---|---|---|---|---|
| 1 | $CD_2Cl_2$ | 8.9 | 0.0167 | 0 | 298 | 2.1(±0.1) | 1.3(±0.1) |
| 2 | $CD_2Cl_2$ | 8.9 | 0.0144 | 0 | 298 | 2.3(±0.1) | 1.3(±0.1) |
| 3 | $CD_2Cl_2$ | 8.9 | 0.0185 | 0 | 298 | 2.0(±0.1) | 1.1(±0.1) |
| 4 | acetone-$d_6$ | 20.7 | 0.0153 | 0 | 298[a] | 2.3(±0.1) | 1.3(±0.1) |
| 5 | acetone-$d_6$ | 20.7 | 0.0137 | 0 | 308[a] | 5.6(±0.5) | 2.9(±0.5) |
| 6 | acetone-$d_6$ | 20.7 | 0.0230 | 0 | 318[a] | 20.(±3.5) | 10.5(±3.5) |
| 7 | acetone-$d_6$ | 20.7 | 0.0085 | 0.0572 | 298 | 2.3(±0.1) | 1.3(±0.1) |
| 8 | acetone-$d_6$ | 20.7 | 0.0105 | 0.187 | 298 | 2.7(±0.2) | 1.6(±0.2) |
| 9 | $CD_3OD$ | 33.6 | 0.0130 | 0 | 298 | *b* | *b* |
| 10 | $CD_3OD$ | 33.6 | 0.0130 | 0 | 323 | *c* | *c* |
| 11 | $CD_3CN$ | 36.8 | 0.0142 | 0 | 298 | 0.031(±0.001) | 0.021(±0.001) |

[a] The activation parameters based on runs 4–6 are $\Delta H^{\ddagger}_1$ = 82.8(±1.2) kJ·mol$^{-1}$, $\Delta H^{\ddagger}_2$ = 79.2(±1.5) kJ·mol$^{-1}$, $\Delta S^{\ddagger}_1$ = −37.4(±3.9) J·K$^{-1}$·mol$^{-1}$, $\Delta S^{\ddagger}_2$ = −54.2(±4.9) J·K$^{-1}$·mol$^{-1}$. [b] No reaction after 24 h. [c] <5% was converted in 24 h.

occasionally revealed two distinct summits; however the control program was able to center and refine during search and index. The space group $P2_12_12_1$ (No. 19) was assigned in all cases on the basis of systematic absences ($h00$, $h \neq 2n$; $0k0$, $k \neq 2n$; $00l$, $l \neq 2n$). All measurements were made with graphite monochromated Mo (**3a**) or Cu (**4a**·2H$_2$O, **5a**) K$\alpha$ radiation and a 2-kW sealed tube generator. Weak reflections ($I < 10.0\sigma(I)$) were rescanned (maximum of 2) and the counts accumulated to assure good counting statistics. For **4a**·2H$_2$O the intensities of three representative reflections, measured after every 150 reflections, declined by 11.00%; hence a linear correction factor was applied to the data. The phenyl and cyclopentadiene rings were refined as rigid groups. All non-hydrogen atoms were refined anisotropically. Idealized hydrogen atoms were included at the calculated positions but were not refined. A correction for secondary extinction was applied (coefficient = 0.877 48 × 10$^{-7}$) in the case of **5a**. The absolute stereochemistry was confirmed in each case by refinement of the enantiomer to a higher $R$ value and correct stereochemistry of the reference carbon known to be $S_C$. Further details are given in Table IX.

**Kinetics for the Arbuzov Dealkylation Step.** Kinetic studies of the Arbuzov dealkylation reaction were carried out in NMR tubes by dissolving solid **3a** in the required amount of solvent. Concentration/time data were obtained by integration of Cp and OMe $^1$H NMR resonances of the reactant **3a** and the products **4a** and **4b**. In a typical experiment 6.61 mg (0.0107 mmol) of **3a** was dissolved in 0.70 mL of acetone-$d_6$ under nitrogen in a preweighed 5-mm NMR tube. The tube was closed with a screw-cap septum seal, mixed until homogeneous using a vortex mixer, and transferred to a thermostated NMR probe. Ten spectra were collected at a time interval of 300 s and then the time interval was increased to 600 s. The reactions were generally followed to completion. The first order rate constants $k_1$ and $k_2$ were obtained by nonlinear least squares regression analysis of the integrated concentration vs time data.

**Synthesis of the Pyrrole-2-carboxaldehyde (*S*)-(1-Phenylethyl)imine Anion (N–N*).** The Schiff base N–N* (N*–N = (*S*)-Ph(Me)C*H—N=CH—$C_4H_3N$-, $C_4H_3N$- = pyrrolyl) was prepared using a modification of the published procedure[32] which avoided the high temperature distillation step. Eqimolar amounts of pyrrole-2-carboxaldehyde (5.444 g, 57.23 mmol) and (*S*)-(phenylethyl)amine (6.988 g, 57.67 mmol) were dissolved into about 100 mL of benzene. p-Toluenesulfonic acid (10 mg) and 50 mL of molecular sieves (activated type 4-A, 4–8 mesh) were added, and the reaction mixture was stirred at room temperature. IR spectroscopy monitored the intensity decrease of $\nu_{C=O}$ at 1664 cm$^{-1}$ and the intensity increase of $\nu_{C=N}$ at 1635 cm$^{-1}$. The reaction was generally complete after stirring for about 6 h. The crude reaction mixture was filtered through a glass frit fitted with a Celite pad. The filtrate was collected and the solvent removed by aspirator and then oil pump vacuum, leaving the product as a pale yellow oil (10.306 g, 91%) which was characterized by the comparison of the NMR and IR data with the published data.[32] IR (neat, cm$^{-1}$): 1638 ($\nu_{C=N}$), 3417 ($\nu_{N-H}$). $^1$H NMR ($CDCl_3$, ppm): 1.54 (Me, d, 6.7 Hz), 4.46 (C*H, q, 6.7 Hz), 6.15 ($H_4$, m), 6.47 ($H_3$, m), 6.65 ($H_5$, m), 7.14–7.33 (phenyl protons), 8.14 (CH=N, s), 9.75 (NH, broad). $^{13}$C NMR ($CDCl_3$, ppm): 24.32 (Me), 68.84 (C*H), 109.39 ($C_4$), 114.58 ($C_3$), 122.06 ($C_5$), 126.52, 126.71, 128.28 ($C_{ortho}$, $C_{meta}$, $C_{para}$), 129.99 ($C_{ipso}$), 144.74 ($C_2$), 150.74 ($C_{CH=N}$). The N–N* anion as obtained as the sodium salt before the preparation of complex **2** by treatment with NaH.[32]

**Table IX. Summary of Crystallographic Data for 3a, 4a·2H$_2$O, and 5a**

| | 3a | 4a·2H$_2$O | 5a |
|---|---|---|---|
| | Crystal Data | | |
| formula | $C_{26}H_{29}CoIN_2O_2P$ | $C_{25}H_{30}CoN_2O_4P$ | $C_{26}H_{29}CoIN_2P$ |
| mol wt | 618.34 | 512.43 | 586.34 |
| cryst syst | orthorhombic | orthorhombic | orthorhombic |
| cryst size (mm) | 0.25 × 0.25 × 0.20 | 0.30 × 0.20 × 0.10 | 0.30 × 0.20 × 0.20 |
| $a, b, c$ (Å) | 13.77(2), 18.08(1), 10.862(6) | 16.692(5), 32.33(2), 9.379(6) | 13.308(4), 17.977(4), 10.790(3) |
| $V$ (Å$^3$) | 2705(4) | 5062(4) | 2581(1) |
| space group | $P2_12_12_1$ (No. 19) | $P2_12_12_1$ (No. 19) | $P2_12_12_1$ (No. 19) |
| $Z$ | 4 | 8 | 4 |
| $D_{calc}$ (g·cm$^{-3}$) | 1.518 | 1.345 | 1.509 |
| $F_{000}$ | 1240 | 2144 | 1176 |
| $\mu$ (cm$^{-1}$) | 18.44 (Mo K$\alpha$) | 64.38 (Cu K$\alpha$) | 156.68 (Cu K$\alpha$) |
| | Data Collection | | |
| temp (K) | 298 | 298 | 298 |
| scan type | $\omega$–$2\theta$ | $\omega$–$2\theta$ | $\omega$–$2\theta$ |
| $\Delta$ (deg) | 1.78 + 0.30 tan $\theta$ | 0.84 + 0.30 tan $\theta$ | 1.15 + 0.30 tan $\theta$ |
| $2\theta_{max}$ (deg) | 45.1 | 100.1 | 120.2 |
| total no. of data | 7680 | 6002 | 4432 |
| no. of unique data | 2052 | 3003 | 2216 |
| no. of obs data | 962 ($I > 3.0\sigma(I)$) | 1112 ($I > 3.0\sigma(I)$) | 873 ($I > 3.0\sigma(I)$) |
| | Refinement | | |
| no. of variables | 138 | 231 | 111 |
| Lorentz polariz trans factors[a] | 0.91–1.00 | 0.61–1.00 | 0.71–1.14 |
| $R$,[b] $R_w$,[c] GOF[d] | 0.046, 0.041, 1.67 | 0.065, 0.047, 1.59 | 0.065, 0.046, 1.83 |
| max/min resd dens (e/Å$^3$) | 0.53/–0.46 | 0.46/–0.48 | 0.81/–0.86 |

[a] Cf. ref 53. [b] $R = \sum||F_o|-|F_c||/\sum|F_o|$. [c] $R_w = [(\sum(|F_o|-|F_c|)^2/\sum wF_o^2)]^{1/2}$. [d] GOF = $(\sum(|F_o|-|F_c|)/\sigma)/(n-m))$ where $n$ = no. of reflections, $m$ = no. of variables, and $\sigma^2$ = variance of $(|F_o|-|F_c|)$.

**Synthesis of ($S_{Co}$,$S_C$)-[($\eta^5$-Cp)Co(N–N*)(PPh(OMe)$_2$)]$^+$I$^-$, 3a.** PPh(OMe)$_2$ (0.1906 g, 1.120 mmol) was added slowly via syringe with stirring under nitrogen to a dark-blue solution of **2a,b** (**2a**/**2b** = 85/15, 0.4541 g, 1.013 mmol) in 30 mL of benzene at room temperature. A deep-red precipitate immediately formed. After stirring for another 5 min, the precipitate was collected on a glass frit, washed with cold benzene (5 × 5 mL), and then dried at room temperature under oil pump vacuum to afford the product as a deep-red powder, 0.4950 g (79%). $^1$H NMR ($CD_3OD$) showed the presence of a single diastereomer, **3a**. **3a** was dissolved into a small amount of $CH_2Cl_2$ and

crystallized by slow diffusion of pentane at −20 °C to give deep-red rectangular plates, mp 84–86 °C, $[\alpha]_{579} = -700$. Due to low transmittance, optical rotations at other wavelengths were not measurable. Anal. Calc for $C_{26}H_{29}N_2O_2PICo$: C, 50.50; H, 4.73; N, 4.53. Found: C, 50.14; H, 4.83: N, 4.40. $^1$H NMR analysis of the residue obtained by removal of solvent from the filtrate under oil pump vacuum showed six Cp peaks which correspond to **3a** (5.40 ppm), **3b** (5.67 ppm), **4a** (4.84 ppm), **4b** (4.71 ppm), **4c** (5.04 ppm), and **4d** (4.96 ppm).

**Synthesis of ($S_{Co}$,($S$,$R_P$),$S_C$)-($\eta^5$-Cp)Co(N–N*)(P(O)(Ph)-(OMe)), 4a,b.** A suspension of 0.4932 g (0.7976 mmol) **3a** in 50 mL of benzene was heated with stirring at 60 °C under a nitrogen atmosphere for 3 h. Removal of solvent by aspirator and then oil pump vacuum left a red, pastelike solid. $^1$H NMR analysis of the crude product showed that the reaction is quantitative and that the two diastereomers **4a**/**4b** are formed with 36% de. Repeated chromatographic separation on 4-mm radial thick-layer silica gel plates (Chromatotron) eluting with methanol/benzene (1:20 v/v) separated a faster moving orange-red zone of **4a**. Removal of solvent gave a red pastelike solid, 0.1748 g (46%). Red plates were obtained by slow diffusion of pentane at −20 °C onto a solution of **4a** in acetone, mp 118–120 °C. $[\alpha]_{579} = -1292$, $[\alpha]_{546} = -321$, $[\alpha]_{436} = +1693$. Anal. Calc for $C_{25}H_{26}N_2O_2PCo{\cdot}2H_2O$: C, 58.60; H, 5.90; N, 5.47. Found: C, 57.19; H, 5.53; N, 5.17. A red, pastelike solid sample of low $R_f$ **4b** was obtained by washing manually separated silica powder containing **4b** with methanol.

**Synthesis of ($S_{Co}$,$S_P$)-[($\eta^5$-Cp)Co(N–N*)(PPhMe$_2$)]$^+$I$^-$, 5a.** $PPhMe_2$ (0.1228 g, 0.8889 mmol) was added slowly under nitrogen via syringe with stirring to a dark-blue solution of **2a,b** (**2a**/**2b** = 85/15, 0.1603 g, 0.3577 mmol) in 10 mL of benzene at room temperature. A brown-red precipitate formed immediately. Stirring was continued for another 5 min, and then the precipitate was collected on a glass frit, washed with cold benzene (5 × 5 mL), and dried at room temperature at oil pump vacuum to give the title complex as a brown-red powder, 0.1564 g (75%). $^1$H NMR showed the prsence of a single diastereomer, **5a**. The crude product was dissolved into a small amount of $CH_2Cl_2$ and crystallized by slow diffusion of hexane at −20 °C to afford black rectangular plates, mp 154–156 °C. $[\alpha]_{579} = -580$. Anal. Calc for $C_{26}H_{29}N_2PICo$: C, 53.26; H, 4.99; N, 4.78. Found: C, 53.20; H, 4.88; N, 4.89.

**Acknowledgment.** We thank the Natural Sciences and Engineering Research Council of Canada (NSERC) for financial support of this work. Z.Z. acknowledges Memorial University for a graduate fellowship.

**Supplementary Material Available:** Tables of bond angles, torsion or conformation angles, bond distances, atomic parameters, and thermal parameters (107 pages). Ordering information is given on any current masthead page.

OM930060W